

## Prompt fission neutron spectra in the $^{235}\text{U}(n,f)$ reaction

B. Mauss<sup>1,2</sup>, J. Taïeb<sup>1,2</sup>, B. Laurent<sup>1</sup>, G. Bélier<sup>1,2</sup>, A. Chatillon<sup>1,2</sup>, D. Étassé<sup>3</sup>, P. Morfouacé<sup>1,2</sup>, O. Roig<sup>1,2</sup>, M. Devlin<sup>4</sup>, J.A. Gomez<sup>4</sup>, R. C. Haight<sup>4</sup>, K. J. Kelly<sup>4</sup>, J.M. O'Donnell<sup>4</sup>, and K.T. Schmitt<sup>5</sup>

<sup>1</sup>CEA, DAM, DIF, F-91297 Arpajon, France

<sup>2</sup>Université Paris-Saclay, CEA, Laboratoire Matière en Conditions Extrêmes, F-91680 Bruyères-le-Châtel, France

<sup>3</sup>LPC Caen, ENSICAEN, Université de Caen, CNRS-CEA, F-Caen, France

<sup>4</sup>P-27, Los Alamos National Laboratory, Los Alamos, New Mexico 87545, USA

<sup>5</sup>ISR-1, Los Alamos National Laboratory, Los Alamos, New Mexico 87545, USA

**Abstract.** Prompt fission neutron spectra (PFNS) are crucial to any neutronic simulation of critical nuclear systems. An experimental setup dedicated to the measurements of PFNS of very high accuracy was developed at the Los Alamos Neutron Science Center (LANSCE) some ten years ago. It allows for the measurement of PFNS for neutron induced fission at the Weapon Neutron Research (WNR) neutron source of the LANSCE. A measurement of the PFNS from the  $^{235}\text{U}(n,f)$  reaction was realized recently and is currently analyzed. Preliminary results are presented here and are compared to present nuclear data evaluations.

### 1 Introduction

Neutrons emitted in fission reactions play a decisive role in many nuclear applications. They can induce new fissions in the nuclear fuel of nuclear reactors, which maintains the nuclear chain reaction. They are a crucial input for nuclear transport codes, with impact on the prediction of core evolution, damage to the vessel and nuclear criticality. These transport codes depend on nuclear data among which the prompt fission neutron spectra (PFNS) are of the utmost importance [1, 2]. In particular, the mean kinetic energy and mean neutron multiplicity can be obtained from PFNS. Their importance is such, that they must be known with an uncertainty better than one percent and of the order of one per thousand, respectively.

Such precision has been achieved for PFNS measurements with thermal neutron impinging on usual actinides, but much less studies have been performed to this day for fission induced by neutrons of higher energy. This holds for  $^{235}\text{U}$ , for which only few data above 1 MeV incoming neutron energy could be used in nuclear data evaluations [3].

Our French-USA collaboration performed an experimental measurement of the PFNS from the  $^{235}\text{U}(n,f)$  reaction. In the following, the experimental method and setup are first described. A short explanation of the analysis steps is then given. Finally, the results obtained are compared to present nuclear data evaluations.

### 2 Experimental method

The experiment was conducted at the Weapon Neutron Research (WNR) installation of the Los Alamos Neutron

Science Center (LANSCE) [4] using the double time-of-flight method to measure the PFNS for neutron incoming energies above 1 MeV. The setup was installed in the experimental flight path 15L, built for the measurement of PFNS at LANSCE. The room contains a "get lost" pit to keep all concrete walls at least 3 m away from the target chamber and thus reduce the background from scattered neutrons [4]. A white neutron source is obtained from a pulsed beam of 800 MeV proton impinging on a tungsten spallation target. The emitted neutrons always get to the fission chamber, 21.5 m away from the spallation target. An incident neutron time-of-flight (ToF) is determined from the time of the beam pulse and the time of a measured fission. The measured incoming neutron energy ranges from 0.7 MeV to about 700 MeV.

The fission chamber is an ionization chamber filled with  $\text{CF}_4$  gas at a pressure of about 100 mbar above the local atmospheric pressure. The chamber contains a stack of 22 cathodes and 11 anodes. On each cathode, a  $^{235}\text{U}$  sample was deposited. The anodes are connected to specifically designed front-end electronics and allow for a good discrimination between fission fragments and alpha particles escaping the  $^{235}\text{U}$  deposits [6–8].

If a fission reaction occurs, prompt fission neutrons can then be measured in the Chi-Nu high energy neutron detector array from LANSCE [4, 5]. It consists of 54 EJ-309 liquid scintillator cells, read by photomultipliers, and arranged on a hemisphere of inner radius 1 m centered on the fission chamber. Each cell has a 17.78 cm diameter and 5.08 cm thickness. The detectors are placed at 9 different angles with six detectors per angle, from  $0^\circ$  to  $150^\circ$  with respect to the beam axis. A second ToF is determined from the time of the fission and the time of a neutron detec-

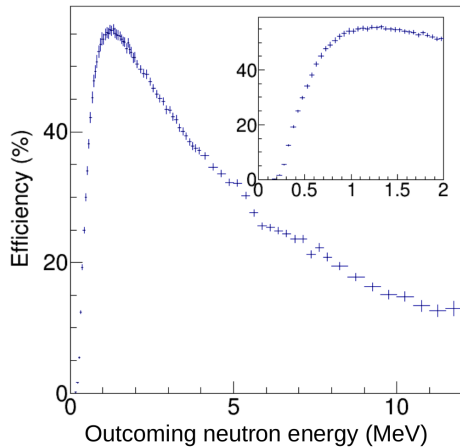


**Figure 1.** Intrinsic neutron detection efficiency as a function of incoming neutron energy of the Chi-Nu liquid scintillator array. The inset shows a zoom of the efficiency curve at low energy.

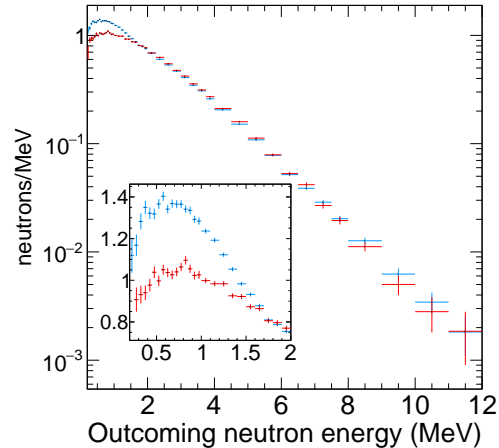


**Figure 2.** Prompt fission neutron spectra obtained at incoming energies of 5.5 MeV (red crosses) and 7.5 MeV (blue crosses). The inset shows a zoom of the low energy part of the distribution. Preliminary data.

tion in the neutron detector, from which the prompt fission neutron kinetic energy is extracted.

The EJ-309 is sensitive to neutrons as well as  $\alpha$  rays, which are selected out by pulse shape analysis techniques (Section 3). The PMT (PhotoMultiplier Tubes) are connected to a dual gain amplifier. The PMT signal is split in two and both legs are shaped through a two-stage Sallen-Key low pass filter. One of the two channels is further amplified. This allows for an increased dynamic range. The non-amplified channel covers high energy deposit in the scintillator while the amplified channel allows for an improved  $\alpha$ /neutron discrimination for smaller signals. The overall detection efficiency is improved, most notably in the low neutron energy range of the PFNS.

An identical chamber containing one  $^{252}\text{Cf}$  deposit, placed in the same conditions as the  $^{235}\text{U}$  chamber, was used for the neutron detection efficiency calibration of the Chi-Nu detectors. The  $^{252}\text{Cf}$  is a spontaneous fissioning nuclide and its PFNS is a so-called standard. The PFNS is reconstructed with Chi-Nu and compared to the standard in order to extract an intrinsic efficiency curve of each liquid scintillator. Figure 1 shows the reconstructed intrinsic efficiency curve of the Chi-Nu liquid scintillator array connected to the dual gain electronics. The fission neutron kinetic energy threshold obtained during this experiment is about 225 keV.

### 3 Analysis and results

The analysis performed here is similar to the one reported in Ref. [8]. Fission events are first selected from the fission chamber charge spectra. The following selection of the prompt fission neutrons is based on the pulse shape characteristics of the PMT's signals which is related to the characteristics of the EJ-309 scintillator light emission time response. A slow light emission component of the scintillator is observed when detecting neutrons and allows for a pulse shape discrimination to discriminate  $\alpha$  rays from neutrons. Second, the correlation between particle energy

deposits in the liquid scintillator and the light output allows the removal of background from scattered neutrons. Indeed, scattered neutrons coming back to the liquid scintillator cell can deposit more energy than they should have from their time-of-flight [8]. The spectrum of selected fission neutrons is finally divided by the efficiency measured with the  $^{252}\text{Cf}$  chamber, giving the PFNS.

PFNS are obtained as a function of incoming neutron energies. Two typical PFNS (preliminary data) are shown on Fig. 2 for incoming neutron energies of 5.5 MeV (red crosses) and 7.5 MeV (blue crosses). The difference between the two spectra is related to the onset of the second chance fission. Second chance fission is allowed when the compound nucleus formed of the incoming neutron and of the target nucleus has enough excitation energy to first emit a neutron and for the remaining excited system to fission. This mechanism is probable only if the remaining excited system possesses an excitation energy above the fission barrier.

In the  $^{235}\text{U}$  case, the second chance fission threshold is around 6 MeV of incident neutron energy. The red crosses, at 5.5 MeV incoming neutron energy, is the PFNS just below second chance fission. The blue crosses, at 7.5 MeV incoming neutron energy, is the PFNS above the second chance fission threshold by 1.5 MeV. We can see on Fig. 2 that the spectra are essentially identical above 1.5 MeV. The difference between the two is the excess of neutrons with energy lower than 1.5 MeV for the PFNS at 7.5 MeV of incoming neutron energy. This excess corresponds to neutrons emitted before the second chance fission.

From the PFNS, we extract the kinetic mean energy of the prompt fission neutrons. In that endeavor, two corrections need to be applied. First, the prompt fission neutrons characteristics of the EJ-309 scintillator light emission time response need to be taken into account. The PFNS are fitted with a Watt distribution between 225 keV and 1.2 MeV. The result of the fits are extrapolated below the threshold down to 0 MeV. The extrapolation provides an approxima-

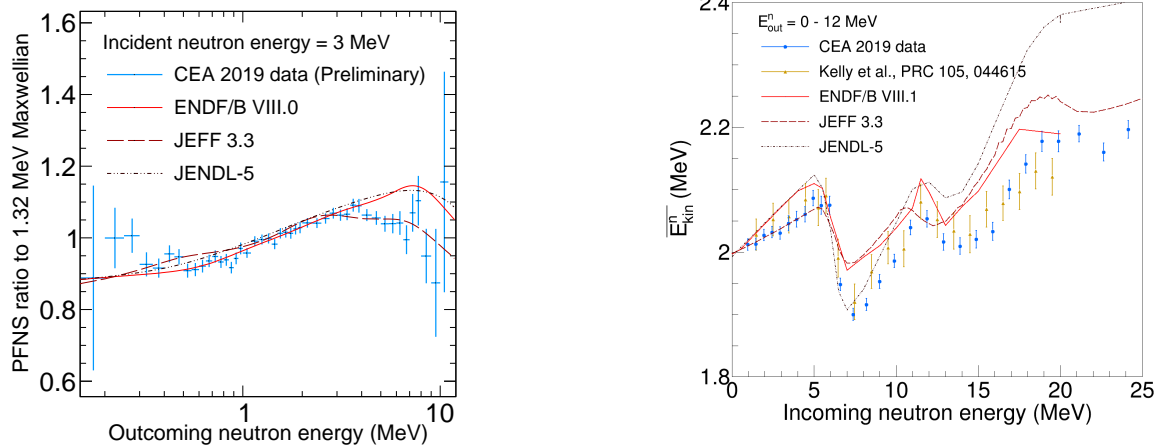


**Figure 3.** Left PFNS ratio to 1.32 MeV Maxwellian as a function of the outcoming neutron energy for an incoming neutron energy of 1 MeV. Right Mean outcoming neutron energy as a function of the incoming neutron energy. Our results (blue circles) are compared to ENDF/B VIII.1, JEFF 3.3 and JENDL-5 nuclear data evaluations, as well as with the data from Ref. [9] (yellow triangles). Preliminary data.

tion to complete the PFNS at low energy and extend our measurement of  $^{252}\text{Cf}$ . The two sets of data are in good range for the extraction of the PFNS mean energy. agreement, which validates the present measurement. The

Second, we take into account the angular distribution. precision of our preliminary data, inferior to the percent, The mean prompt ssion neutron energy is extracted per shows that the nalized data should provide constraints to polar angle per incoming neutron energy. It is tted by evaluations and reduce their uncertainties.

a polynomial of order 4. The angular distribution of the PFNS mean energy is extrapolated to regions not covered by the Chi-Nu array. The obtained integral of the PFNS mean energy angular distribution provides a realistic mean energy per incoming neutron energy.

#### 4 Comparison to evaluations

In order to better observe the discrepancy between data and evaluations, the ratios of PFNS to a 1.32 MeV Maxwellian distribution are plotted. Figure 3 left shows, few MeV of incident neutron energies, where evaluations for a mean incoming neutron energy of 1 MeV, the comparison between our preliminary data and the nuclear data evaluations ENDF/B VIII.0, JEFF 3.3 and JENDL-5. The agreement is very good overall, though some data analysis remains to be done. We see that there is an agreement over most of the spectrum, at the exception of prompt ssion neutron energies below 0.3 MeV and above 7 MeV, where our data shows an excess of neutrons.

The prompt ssion neutron energy averaged over 0 to 12 MeV of ssion neutron energy is plotted as a function of incoming neutron energy on Fig. 3, right. Comparing our data to evaluations, we see that there are large discrepancies between the nuclear data evaluations above 2 MeV of incoming neutron energy. Below 5 MeV, our preliminary data agrees more with JEFF 3.3. Between 5 and 12 MeV it agrees more with JENDL-5, and above with ENDF/B VIII.0. Recent data from Ref. [9], also obtained at Los Alamos using Chi-Nu, is shown on the figure. There are several differences in the setup of Ref. [9], including the ssion chamber and the use of Li-glass detector array for the detection of low energy prompt ssion neutrons, as well as a different analysis technique, not relying on the

#### 5 Conclusion and outlook

In conclusion, we measured prompt ssion neutron spectra in the  $^{235}\text{U}(n,f)$  reaction for incident neutron energies between 0.7 MeV and 700 MeV on the WNR installation at LANSCE. The measurement was done with respect to the standard  $^{252}\text{Cf}(sf)$  PFNS. The preliminary results compare well with the ENDF/B VIII.0, JEFF 3.3 and JENDL-5 nuclear data evaluations at low incident neutron energies. Once nalized, they should provide constraints above a few MeV of incident neutron energies, where evaluations are currently in disagreement.

In a similar experiment of  $^{239}\text{Pu}$  [8], the neutron multiplicity was also extracted [10]. The extraction of the neutron multiplicity from our data of  $^{235}\text{U}$  is currently in progress. As an outlook, a new liquid scintillator array, VERSA-neutron energies below 0.3 MeV and above 7 MeV, where our data shows an excess of neutrons.

As an outlook, a new liquid scintillator array, VERSA-tile Neutron DETector Array (VENDETA), has been developed by the CEA to be used for PFNS measurements at LANSCE. Built to improve the time resolution and decrease the light detection threshold, it should increase the neutron detection efficiency, and in particular improve the quality of the PFNS at low and high energies. A PFNS measurement on the  $^{235}\text{U}(n,f)$  reaction was done in autumn 2022. It should be followed in coming years by PFNS measurement of  $^{240}\text{Pu}$  and  $^{239}\text{Pu}$ .

#### References

[1] Y. Penelieu et al., Nuclear Data Sheets **118**, 459 (2014)  
 [2] R. Capote et al., Nuclear Data Sheets **131**, 1-106 (2016)

- [3] D. Neudecker et al., Nuclear Data Sheets **148**, 293-311 (2018)
- [4] M. Devlin et al., Nuclear Data Sheets **148**, 322-337 (2018)
- [5] B. A. Perdue et al., Nucl. Data Sheets **119**, 371 (2014)
- [6] J. Taïebet et al., Nuclear Instruments and Methods in Physics Research, **833**, 1-7 (2016)
- [7] B. Laurent et al., Nuclear Instruments and Methods in Physics Research, **990**, 164966 (2021)
- [8] P. Marini et al., Physical Review **C101**, 044614 (2020)
- [9] K. J. Kelly et al., Physical Review **C105**, 044615 (2022)
- [10] P. Marini et al., arXiv:2109.14330 [nucl-ex] (2021)